

H/D isotope exchange reaction of SiH₃ with SiD₄ and SiD₃ with SiH₄: Evidence for hydride stripping reaction

W. D. Reents Jr. and M. L. Mandich

Citation: *The Journal of Chemical Physics* **93**, 3270 (1990); doi: 10.1063/1.458860

View online: <http://dx.doi.org/10.1063/1.458860>

View Table of Contents: <http://scitation.aip.org/content/aip/journal/jcp/93/5?ver=pdfcov>

Published by the [AIP Publishing](#)

Articles you may be interested in

[H/D isotopic exchange between water molecules at ice surfaces](#)

J. Chem. Phys. **121**, 2765 (2004); 10.1063/1.1770548

[Strong isotope effects in the dissociation kinetics of Si–H and Si–D complexes in GaAs under ultraviolet illumination](#)

Appl. Phys. Lett. **75**, 112 (1999); 10.1063/1.124292

[The isotope exchange reactions H₂+D₂HD+D₂ and D₂+H₂HD+H₂ in the temperature range 200–300 K](#)

J. Chem. Phys. **75**, 1201 (1981); 10.1063/1.442168

[Calculation of H/D Kinetic Isotope Effects for the Reactions of Trifluoromethyl Radicals with SiH₄](#)

J. Chem. Phys. **54**, 1919 (1971); 10.1063/1.1675119

[Lifetimes and Total Transition Probabilities for NH, SiH, and SiD](#)

J. Chem. Phys. **51**, 520 (1969); 10.1063/1.1672027



H/D isotope exchange reaction of SiH_3^+ with SiD_4 and SiD_3^+ with SiH_4 : Evidence for hydride stripping reaction

W. D. Reents, Jr. and M. L. Mandich
AT&T Bell Laboratories, Murray Hill, New Jersey 07974

(Received 10 January 1990; accepted 22 May 1990)

We have measured the reaction rates and product distributions for $\text{SiH}_x\text{D}_{3-x}^+$ reactions with SiH_4 and SiD_4 . The measured reaction rates for SiH_3^+ and SiD_4 ($26.1 \pm 1.0 \times 10^{-10}$ cc/molecule s) and for SiD_3^+ and SiH_4 ($23.1 \pm 1.0 \times 10^{-10}$ cc/molecule s) are greater than the calculated Langevin collision rate ($12.3\text{--}12.4 \times 10^{-10}$ cc/molecule s). Also, the product distribution observed for H/D exchange is nonstatistical. Dual, competing reaction mechanisms are invoked to account for these observations: reaction via formation of an ion-molecule complex and reaction via long-range hydride stripping. Using an expected product distribution calculated from reaction thermochemistries, the relative contributions of the two mechanisms is obtained for each reaction examined. The reaction rate for the ion-molecule complex mechanism is calculated to be at the Langevin collision rate within experimental error. The reaction rate for the stripping mechanism varies from $1\text{--}4 \times 10^{-10}$ cc/molecule s (10–30% of the Langevin collision rate) for the mixed isotope ions SiH_2D^+ and SiHD_2^+ to $12\text{--}18 \times 10^{-10}$ cc/molecule s (100%–150% of the Langevin collision rate) for the isotopically pure ions SiH_3^+ and SiD_3^+ . The faster than Langevin reaction rates lower the expected low field mobility of SiH_3^+ in silane plasmas by 70% to ~ 340 cm² Torr/V s.

I. INTRODUCTION

Silane chemical vapor deposition is used in the electronics industry to deposit silicon films with superior purity than bulk silicon. Use of a plasma [plasma enhanced chemical vapor deposition (PECVD)] allows for lower deposition temperatures for temperature sensitive features. The events in plasmas which lead to silicon deposition are complex with many factors coupled together; changing an operating parameter will have a somewhat unpredictable result on the film quality and deposition rate. Events in plasmas and on surfaces are being modeled to understand how the different parameters are coupled and thereby aid in optimizing the deposition process.^{1–4} A major goal is to uncover the mechanism responsible for the growth of deleterious hydrogenated silicon microparticles in the gas phase. Formation of this silicon “dust” is currently a major problem that will become more devastating as device features shrink.^{5–6}

We have previously examined the gas phase ion chemistry of many bare and hydrogenated silicon cluster cations with silane^{7–10} with the intent of finding an ion/molecule reaction pathway leading to formation of silicon dust in silane plasmas. These studies have provided product distributions and reaction rates which are vital to models of the silane plasma chemistry. Reactions of the ions with silane produce hydrogenated silicon clusters, Si_mH_n^+ , containing no more than six silicon atoms. Thus far we have not found an ionic pathway for production of large gas phase hydrogenated silicon clusters in silane plasmas.

The ionic mobility within the plasma determines the ion residence time and energy, characteristics which are vital to a complete understanding of the plasma.¹¹ The most abundant ion in the plasma, SiH_3^+ , has been observed to react with SiH_4 at a rate greater than the collision rate due to a long range hydride stripping reaction. This high reaction

rate has not been accounted for in silane plasma models but would lower the expected diffusion rate and thereby increase the residence time of SiH_3^+ in the plasma.

In this study we have obtained the relative contributions of the hydride stripping reaction vs the ion-molecule complex formation reaction for thermal (300 K) ions in the observed hydride exchange reaction



Isotopic labeling of the silicon or hydrogen was used to differentiate the two mechanisms. For a pure stripping mechanism, statistical hydrogen isotopic scrambling will not occur, whereas a pure complex formation mechanism would have a statistical distribution of isotopes in the product ions. Experimentally we observe all possible mixed and unmixed isotopic products with a preferred formation of the isotopically unmixed ion, SiH_3^+ or SiD_3^+ , indicating that the two mechanisms compete. Using information from phase space calculations and high level *ab initio* calculations,¹² we have estimated the rates for each mechanism. The rate for hydride exchange via the complex formation mechanism is between 75% and 90% of the Langevin collision rate, whereas the rate of the stripping mechanism exceeds the classical collision rate for isotopically pure reactant ions.

II. EXPERIMENTAL

The studies were performed with a Nicolet FTMS-1000 Fourier transform mass spectrometer modified to include a differentially pumped dual trapped ion cell. Silane (Scott, 99.99%) and SiD_4 (MSD, 99.7 + at %) were admitted to different sides of the differentially pumped chamber. Ions were formed by electron impact with 14 eV electrons to minimize fragmentation and reduce the percentage of ions with excess energy. Ions were transferred from the trapped

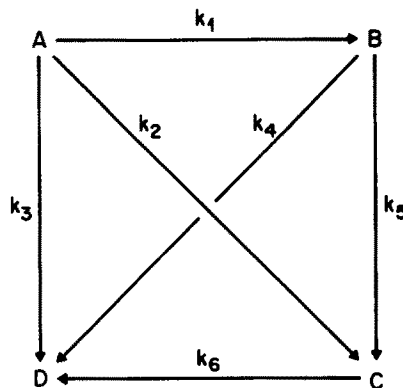
ion cell in which they were formed, through a 2 mm conduction limit, to the second trapped ion cell for reaction. Unwanted ions were ejected by standard double resonance techniques to isolate the reactant ion SiH₃⁺ or SiD₃⁺ for further study. The conduction limit also allowed some gases to transfer from one cell to the other, thereby complicating the kinetics study. This problem was minimized by adjusting the pressures to ensure a greater than 40:1 ratio of the reactant neutral to the interfering neutral. Other conditions were: 3.2–4.2 × 10⁻⁷ Torr total pressure; 32k to 64k data points; 1 V trapping voltage; 100 spectra summed; trapping times of 0.005 to 3 s.

The ion gauge pressure readings were corrected to absolute pressures so that observed reaction rates could be converted to absolute reaction rates. Pressure corrections were made by comparing our measured rates for reaction of CH₃⁺ and CH₄⁺ with CH₄ to literature values and correcting the ion gauge response factor using the molecular polarizability of silane and methane.¹³ Electron ionization energy was a crucial factor in this study. For energies greater than 14 eV, nonexponential decay of the SiH₃⁺/SiD₃⁺ reactant ions was observed. This is due to excess energy in the ion which is observed to slow down the reaction. In some studies, thermalization of the ions through collisions might be possible, but in this experiment the facile reactions (at or near the collision rate) and the difficulty of the experimental setup precluded such an option.

A. Kinetic evaluation

The isotopic exchange reactions involve both parallel and sequential formation of product ions as shown in scheme 1.

The kinetic expression for three sequential reactions have been derived.¹⁴ For four sequential reactions as in scheme 1,



the kinetic expressions are similar. They are presented here for the reader's convenience. For the initial reactant ion *A*:

$$A = A_0 e^{-(k_1 + k_2 + k_3)t}, \quad (2)$$

where *A* is the reactant ion intensity [SiH₃⁺ in reactions (7)–(12) or SiD₃⁺ in reactions (13)–(18)], *A*₀ is the initial intensity of *A*, and *k*₁, *k*₂, and *k*₃ are the reaction rates shown in scheme 1 [they represent the reaction rates for reactions (7)–(9) or (13)–(15), respectively]. For *B*, the kinetic expression is

$$B = \frac{k_2 A_0}{[(k_4 + k_5) - (k_1 + k_2 + k_3)]} (e^{-(k_1 + k_2 + k_3)t} - e^{-(k_4 + k_5)t}), \quad (3)$$

where *B* is the reactant ion intensity [SiH₂D⁺ in reactions (7)–(12) or SiHD₂⁺ in reactions (13)–(18)] and *k*₄ and *k*₅ represent the reaction rates shown in scheme 1 [they also represent the reaction rates for reactions (10)–(11) or (16)–(17), respectively]. The kinetic equation for *C* is

$$C = A_0 \left\{ \frac{k_1 + \frac{k_2 k_4}{(k_4 + k_5) - (k_1 + k_2 + k_3)}}{k_6 - (k_1 + k_2 + k_3)} e^{-(k_1 + k_2 + k_3)t} + \frac{\frac{k_2 k_4}{(k_4 + k_5) - (k_1 + k_2 + k_3)}}{-k_6 + (k_4 + k_5)} e^{-(k_4 + k_5)t} - \left[\frac{k_1 + \frac{k_2 k_4}{(k_4 + k_5) - (k_1 + k_2 + k_3)}}{k_6 - (k_1 + k_2 + k_3)} + \frac{\frac{k_2 k_4}{(k_4 + k_5) - (k_1 + k_2 + k_3)}}{-k_6 + (k_4 + k_5)} \right] e^{-k_6 t} \right\}, \quad (4)$$

where *C* is the reactant ion intensity [SiHD₂⁺ in reactions (7)–(12) or SiH₂D⁺ in reactions (13)–(18)] and *k*₆ represents the reaction rate shown in scheme 1 (it also represents the reaction rate for either reaction (12) or (18)). In fitting Eq. (4), the standard deviation of the variables *k*₁, *k*₄, and *k*₆ are minimized to obtain the best fit in the tables. The other variables are set equal to the values obtained from fits to Eqs. (2)–(3). Finally, the rate expression for the final ion, *D*, is

$$D = A_0 \left(1 - \left[\frac{k_1 + \frac{k_2 k_4}{(k_4 + k_5) - (k_1 + k_2 + k_3)}}{k_6 - (k_1 + k_2 + k_3)} e^{-(k_1 + k_2 + k_3)t} + \frac{\frac{k_2 k_4}{(k_4 + k_5) - (k_1 + k_2 + k_3)}}{-k_6 + (k_4 + k_5)} e^{-(k_4 + k_5)t} - \left[\frac{k_1 + \frac{k_2 k_4}{(k_4 + k_5) - (k_1 + k_2 + k_3)}}{k_6 - (k_1 + k_2 + k_3)} + \frac{\frac{k_2 k_4}{(k_4 + k_5) - (k_1 + k_2 + k_3)}}{-k_6 + (k_4 + k_5)} \right] e^{-k_6 t} \right] \right). \quad (5)$$

These equations assume no back reaction occurs. In practice, this is not correct, but it is minimized through use of the differentially pumped dual cell to produce a >40:1 ratio of reactant neutral to neutral from which the reactant ion was derived. A slight residual back reaction was removed for ions *A*, *B*, and *C* by adding the term $x D_0$ to the kinetic equation which accounts for the equilibrium of the ions with the final product ion. This simply sets the equilibrium long time value of an ion to a fraction of the intensity of *D*. A slower reaction of *D* with silane to produce Si₂H₅⁺ or Si₂D₅⁺ is also present. A simpler rate expression for *D* is used:

$$D = Ae^{-(k_1 + k_2 + k_3)t} + Be^{-(k_4 + k_5)t} + Ce^{-k_6t} + De^{-k_x t}, \quad (6)$$

where k_x is the rate for formation of Si₂(H/D)₅⁺. These preexponential factors are not evaluated in terms of kinetic parameters; this equation is merely used to demonstrate a fit with the evaluated reaction rates. These equations are then fit to the intensity variations with time to extract the kinetic information reported. The rate constants in Eqs. (2)–(6) are pseudo-first-order because the neutral reactant (SiD₄ or SiH₄) is present in great excess relative to the reactant ions. The true bimolecular rate constant is obtained through dividing the observed rate constant by the absolute pressure of SiD₄.

The four kinetic equations above are insufficient to determine the six reaction rates k_1 – k_6 . The product distributions are used as additional information to fully evaluate the rate constants.

III. RESULTS

A differentially pumped dual trapped ion cell of a Fourier transform ion cyclotron resonance mass spectrometer is used to study the H/D exchange reactions (7)–(12) and (13)–(18).

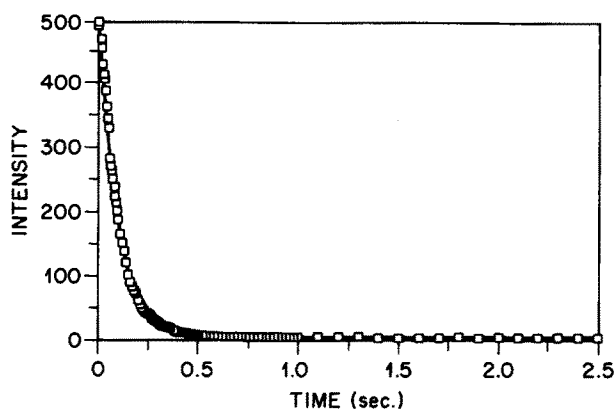
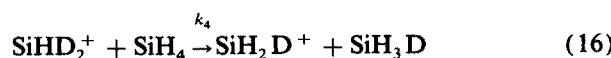
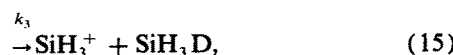
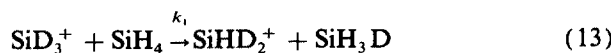
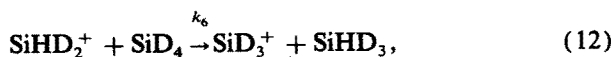
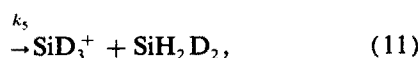
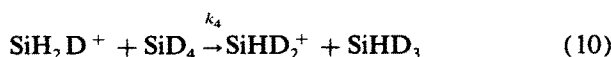
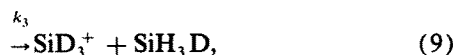
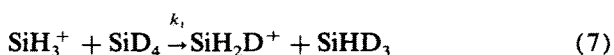
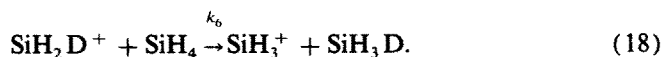
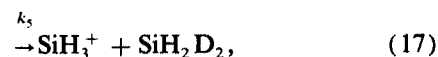


FIG. 1. Time plot for the intensity variation of SiH₃⁺ in its reaction with SiD₄ from reactions (7)–(9). The solid line is the kinetic fit to the intensity using Eq. (2) and considering a small equilibrium contribution as discussed in Sec. II A.



The ion intensities as a function of time for reactions (7)–(12) and (13)–(18) are plotted in Figs. 1–4 and 5–7, respectively. Superimposed on the ion plots are the calculated intensities which have been fit to the kinetic equation discussed in Sec. II A. Extracted kinetic parameters for a reactant ion were used to constrain kinetic fits of each product ion. The fitted rates are presented in Table I along with the calculated Langevin collision rate. Also presented in Table I are our previously reported reaction rates for isotopically labeled ²⁹SiH₃⁺ and ²⁹SiD₃⁺ with SiH₄ and SiD₄, respectively.

Product distributions were calculated by phase space theory,^{15,16} statistical mixing of the isotopes, and reaction energies, ΔG_{rxn} . The results of these calculations along with the observed product distributions are presented in Table II.

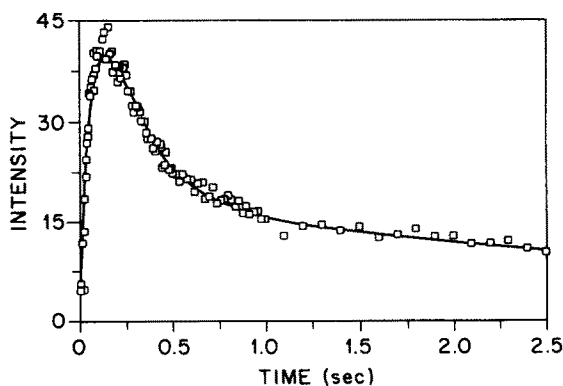


FIG. 2. Time plot for the intensity variation of SiH₂D⁺ in its formation from reaction of SiH₃⁺ with SiD₄ and its reaction with SiD₄ from reactions (7)–(11). The solid line is the kinetic fit to the intensity using Eq. (3) and considering a small equilibrium contribution as discussed in Sec. II A.

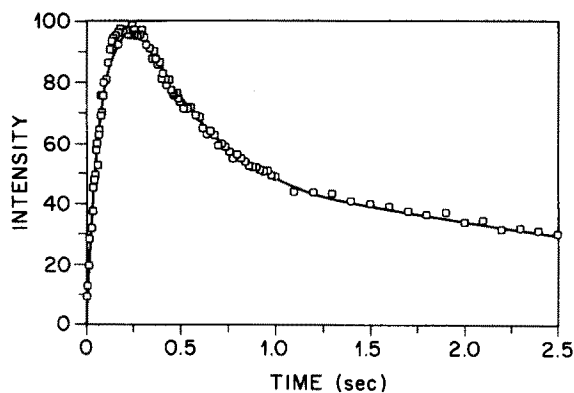


FIG. 3. Time plot for the intensity variation of SiHD_2^+ in its formation from reactions of SiH_3^+ and SiH_2D^+ with SiD_4 and its reaction with SiD_4 from reactions (7)–(12). The solid line is the kinetic fit to the intensity using Eq. (4) and considering a small equilibrium contribution as discussed in Sec. II A.

IV. DISCUSSION

Typically, ion-molecule reactions proceed through an intermediate complex which is bound by ion-dipole forces. For the reaction of $\text{Si}(\text{D}/\text{H})_3^+$ with $\text{Si}(\text{H}/\text{D})_4$ a symmetric, strongly bound hydrogen bridged complex forms (Fig. 8) with a calculated binding energy of 35 kcal/mol.¹² Facile hydrogen/deuterium exchange occurs through a readily accessible transition state (T_1), lying 18 kcal/mol below the energy of the reactants. Since this transition state is well below the transition states leading to products (T_2) or back to reactants, there is a complete mixing of the isotopes resulting in a distribution of isotopically labeled products.¹² Calculated product distributions based upon a simple statistical mixing compares well with the more sophisticated phase space and thermodynamic calculations in Table II. However, there is poor agreement with the experimentally observed distributions. Furthermore, the absolute reaction rates for these reactions exceed the Langevin collision rate in some cases by a factor of 2.

The product distribution discrepancies in Table II can

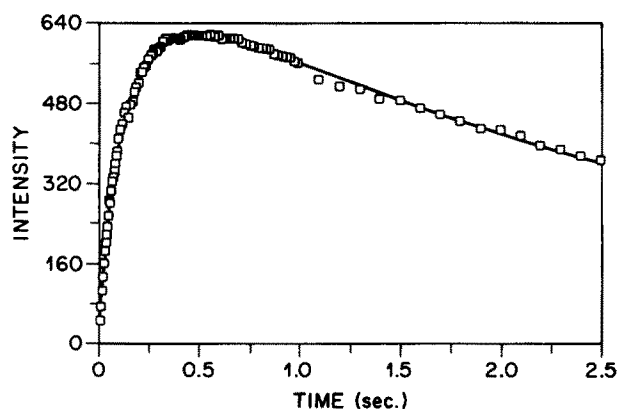


FIG. 4. Time plot for the intensity variation of SiD_3^+ in its formation from reactions of SiH_3^+ , SiH_2D^+ , and SiHD_2^+ with SiD_4 from reactions (7)–(12). The solid line is the kinetic fit to the intensity using Eq. 6.

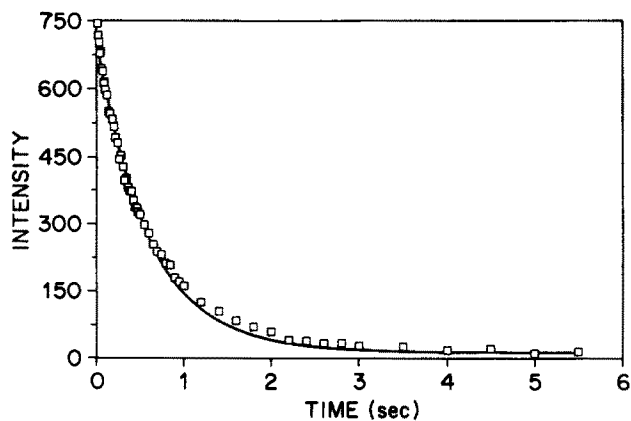


FIG. 5. Time plot for the intensity variation of SiD_3^+ in its reaction with SiH_4 from reactions (13)–(15). The solid line is the kinetic fit to the intensity using Eq. (2) and considering a small equilibrium contribution as discussed in Sec. II A.

be rationalized in terms of a stripping reaction mechanism.^{17,18} In a stripping reaction, transfer of a small particle (e.g., electron, H^+ , H , or H^-) occurs over a distance greater than that required for complex formation. Also unlike complex formation, there is no momentum transfer between the ion and neutral. Thus, stripping reactions are known to efficiently produce thermal ions from a fast ion beam. The stripping reaction has been observed by Mayer and Lampe with an ion beam apparatus for SiH_3^+ reacting with SiD_4 ¹⁹ and $\text{CH}_3\text{SiH}_2^+$ reacting with CH_3SiD_3 .²⁰ In our experiments the stripping mechanism competes with complex formation to produce the convoluted distributions.

The product distribution observed by Lampe and Mayer for reactions (7)–(9) is reproduced in Table III for an ion beam apparatus as a function of reactant ion energy.¹⁹ Only SiD_3^+ and SiHD_2^+ were observed; both SiH_2D^+ and SiH_3^+ were obscured by the primary SiH_3^+ beam. The intensity of SiD_3^+ relative to SiHD_2^+ is significantly less than our result (2:1 vs 6:1). This disagreement with our observations (Table II) lies in the lack of momentum transfer for the

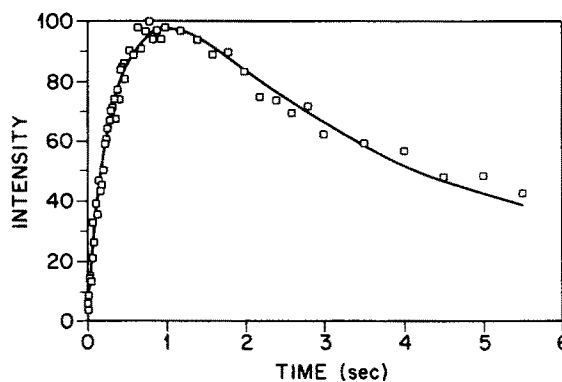


FIG. 6. Time plot for the intensity variation of SiHD_2^+ in its formation from reaction of SiD_3^+ with SiH_4 and its reaction with SiH_4 from reactions (13)–(17). The solid line is the kinetic fit to the intensity using Eq. (3) and considering a small equilibrium contribution as discussed in Sec. II A.

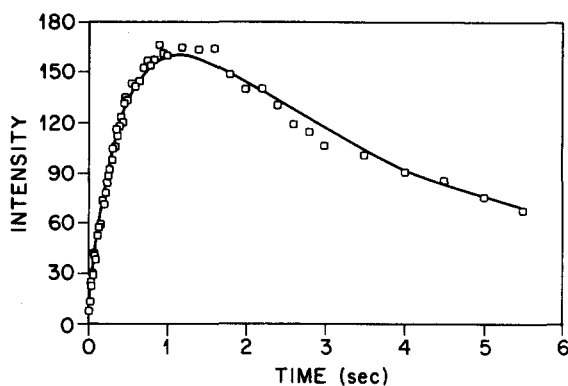


FIG. 7. Time plot for intensity variation of SiH_2D^+ in its formation from reactions of SiD_3^+ and SiHD_2^+ with SiH_4 and its reaction with SiH_4 from reactions (13)–(18). The solid line is the kinetic fit to the intensity using Eq. (4) and considering a small equilibrium contribution as discussed in Sec. II A.

hydride stripping reaction. The ion beam apparatus inefficiently extracted low velocity ions from the reaction tube resulting in a proportionally enhanced signal of SiHD_2^+ .²¹

The complex formation reaction rate cannot be extract-

TABLE I. Estimated reaction rates for complex formation and stripping mechanisms.

Reactants	Reaction rate ($\times 10^{10}$ cc/molecule s) ^f			
	k_{total}	k_{complex}^a	$k_{\text{stripping}}^b$	k_{Langevin}^c
$\text{SiH}_3^+ + \text{SiD}_4$	26.1 ± 1.0	8.2 ± 1.1	18.1 ± 2.1	12.3
$\text{SiH}_2\text{D}^+ + \text{SiD}_4$	14.4 ± 1.0	$14.9_{-4.9}^{+1.0}$	$1.4_{-1.4}^{+4.98}$	12.2
$\text{SiHD}_2^+ + \text{SiD}_4$	11.2 ± 1.0	...	4 ± 3^g	12.1
$\text{SiD}_3^+ + \text{SiH}_4$	23.1 ± 1.0	11.2 ± 2.1	12.1 ± 3.1	12.4
$\text{SiHD}_2^+ + \text{SiH}_4$	15.0 ± 1.0	$13.3_{-3.7}^{+2.7}$	$3.6_{-3.6}^{+4.7}$	12.5
$\text{SiH}_2\text{D}^+ + \text{SiH}_4$	10.3 ± 1.0	...	3 ± 3^g	12.6
$^{29}\text{SiH}_3^+ + \text{SiH}_4$	11 ± 1^d	$(12.5)^e$	5^e	12.5
$^{29}\text{SiD}_3^+ + \text{SiD}_4$	8.5 ± 0.7^d	$(12.0)^e$	2.5^e	12.0

^a Complex formation rate for the mixed H/D exchange reactions is calculated based upon the expected fraction of their formation from Table II compared with the observed fraction of their formation. In these instances the single exchange product fraction is divided by the thermodynamic product fraction and multiplied by the total rate. Reactions whose k_{complex} is omitted do not have a unique nonstripping reaction product.

^b This is calculated from the total measured reaction rate less the calculated complex reaction rate plus the rate for back reaction which cannot be observed experimentally.

^c Langevin ion-molecule collision rate, $2\pi q(\alpha/\mu)^{1/2}$.

^d From Ref. 10. Note that these rate constants do not include the back reaction of the complex formation pathway. So that these values may be compared with the other k_{total} , one half of k_{Langevin} should be added to account for the unobserved back reaction.

^e The complex formation reaction rate cannot be calculated; it is assumed to be equal to one half of the Langevin collision rate (this is the experimentally observable part of the complex formation pathway). That value was subtracted from k_{total} to obtain $k_{\text{stripping}}$. Thus k_{complex} is assumed to equal k_{Langevin} .

^f Listed errors are relative. Absolute errors are $\pm 20\%$.

^g Estimated by taking the thermodynamic calculated distribution for formation of SiH_3^+ or SiD_3^+ , multiplying by k_{Langevin} to get an estimate for the observable k_{complex} , and subtracting k_{total} .

ed from the total reaction rate solely through kinetic analysis. However, if the product distribution for complex formation can be estimated, then its absolute reaction rate can be calculated based upon the product distribution and formation rate of a nonstripping reaction product. For Table II, the observed product ratios of SiH_2D^+ to SiHD_2^+ for reactions (7)/(8) and (13)/(14) agree within experimental error with the calculated values. Using the thermodynamic distributions for the products of reactions (7), (10), (13), and (16), the calculated reaction rates for complex formation and stripping are shown in Table I. [Reactions (7) and (13) were used rather than (8) and (14) because of the smaller relative error in the distributions.]

There are several observations to be highlighted concerning the observed reaction rates. First, complex formation occurs at the Langevin reaction rate (within experimental error). This observation increases our confidence of the results. Second, k_{total} decreases linearly with decreasing number of labeled atoms in the ion. This is a combination of our reduced ability to monitor the complex formation reaction with decreasing isotopic label and a smaller $k_{\text{stripping}}$. Third, $k_{\text{stripping}}$ is comparable to or greater than k_{complex} for the isotopically pure reactant ions but diminishes significantly when the isotopically mixed ions are reacted [reactions (10) and (11) and (16)–(18)]. This may be due to the reduced free energy of reaction (cf. Table IV) for these latter reactions. The reactant ion must approach closer to the neutral to overcome an equivalent energy barrier. Note that $k_{\text{stripping}}$ for the ^{29}Si labeled reactants are comparable to those for the isotopically mixed ions SiH_2D^+ and SiHD_2^+ . Finally, the stripping reaction occurs most readily for reaction (7). Transfer of the lighter H^- in reaction (13) would be expected to proceed more rapidly; even ΔG_{rxn} favors reaction (13). We have no explanation at present for this discrepancy. In contrast, with the ^{29}Si labeled reactants the perdeuterated system has the expected slower k_{total} and $k_{\text{stripping}}$ compared with the per-protiated system. Note that $k_{\text{stripping}}$ for the ^{29}Si labeled reactions, which are thermoneutral, are comparable to $k_{\text{stripping}}$ for the slightly exothermic SiH_2D^+ and SiHD_2^+ reactions.

The rapid reaction rate of SiH_3^+ with SiH_4 will influence the results of modeling silane plasma chemistry. The current low-field mobility estimate of $1180 \text{ cm}^2 \text{ Torr/V s}$ for SiH_3^+ is too high due to an underestimation of this hydride exchange reaction rate.⁴ We have recalculated the low-field mobility using the relation⁴

$$\mu P = \frac{6.36 \times 10^{-24}}{(mkT)^{1/2} Q}, \quad (19)$$

where μP is the low field mobility, m is the mass of the ion in kg/mol, k is the Boltzman constant in Joules, T is the temperature in Kelvin, and Q is the reaction cross section of the ion given by

$$Q = kv, \quad (20)$$

where k is the bimolecular reaction rate constant and v is the ion velocity in cm/s.²² From our measured reaction rate for SiH_3^+ of $2.2 \times 10^{-9} \text{ cc/molecule s}$ at room temperature the calculated low field mobility is $340 \text{ cm}^2 \text{ Torr/V s}$ assuming

TABLE II. Product distributions^a for H/D exchange.

Reactants	Product ion	Distribution (%)			
		Observed	Phase space	Statistical	Thermodynamic ^b
$\text{SiH}_3^+ + \text{SiD}_4$	SiH_3^+	...	0.8	2.9	2.3
	SiH_2D^+	11 ± 1	33	34	35
	SiHD_2^+	13 ± 5	54	51	54
	SiD_3^+	76 ± 6	12	11	8.0
$\text{SiH}_2\text{D}^+ + \text{SiD}_4$	SiH_2D^+	...		14	13
	SiHD_2^+	59 ± 12		57	57
	SiD_3^+	41 ± 12		29	30
$\text{SiHD}_2^+ + \text{SiD}_4$	SiHD_2^+	...		43	43
	SiD_3^+	100		57	57
$\text{SiD}_3^+ + \text{SiH}_4$	SiD_3^+	...	3.1	2.9	2.1
	SiHD_2^+	14 ± 2	36	34	29
	SiH_2D^+	12 ± 10	50	51	57
	SiH_3^+	74 ± 12	10	11	11
$\text{SiHD}_2^+ + \text{SiH}_4$	SiHD_2^+	...		14	13
	SiH_2D^+	48 ± 10		57	54
	SiH_3^+	52 ± 10		29	33
$\text{SiH}_2\text{D}^+ + \text{SiH}_4$	SiH_2D^+	...		43	42
	SiH_3^+	100		57	58

^aThese are the expected equilibrium distributions based upon the free energy of reaction. The enthalpies of reaction are the differences in zero point energy from *ab initio* calculations. The reaction entropies were obtained from the scaled rotational and vibrational constants derived from *ab initio* calculations (Ref. 23). Only vibrational frequencies less than 1000 cm^{-1} were considered since they represented >95% of the vibrational entropy.

^bBased on free energy of reaction, Table IV.

a thermally averaged cross section. This value is based on collisions which equilibrate the kinetic energy of the ion. However, the hydride stripping mechanism, which is a significant fraction of the total reaction, forms an ion fully thermalized with the background gas and a neutral with the kinetic energy of the reactant ion. Thus the average kinetic energy and the low field mobility may be even lower. Nevertheless, this value greatly reduces the ambipolar diffusion loss of SiH_3^+ from the plasma thereby increasing the expected concentration of SiH_3^+ and its reaction progeny in the plasma.

Low field mobilities for all Si_xH_y^+ ions in silane plasmas may be overestimated. For example, complex formation of

ions such as Si^+ , SiH^+ , and SiH_2^+ with SiH_4 have been found to occur with unit efficiency even where the forward reaction efficiency is much less. Formation of a complex causes thermalization of the ion even where this complex falls apart to reactants, thus lowering its mobility.

V. CONCLUSIONS

The hydride exchange reaction of SiH_3^+ with SiH_4 occurs at greater than the Langevin collision rate. Reaction via a conventional collision complex occurs at or near the collision rate. A second mechanism involving hydride stripping at long distance is also present. The combination of the two mechanisms yields an observable rate greater than the collision rate. Through isotopic labeling, the two mechanisms were differentiated. The hydride stripping mechanism ac-

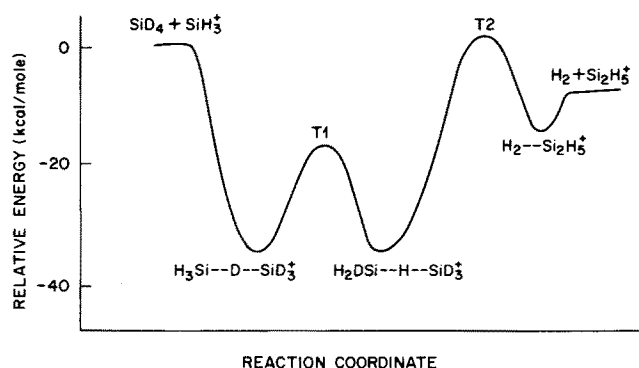


FIG. 8. Potential energy surface for reaction of SiH_3^+ with SiD_4 from Ref. 16. H/D exchange between the low energy complexes occurs via transition state T1 which is 18 kcal/mol below the reactants energy.

TABLE III. Product distribution^a observed in ion beam experiments on the reaction of SiH_3^+ with SiD_4

Product	Collision energy (eV)				
	0.54	1.07	2.15	3.22	4.30
SiD_3^+	68	76	86	83	88
SiHD_2^+	32	24	14	17	12
SiH_2D^+	obscured by primary ion beam ^b				
SiH_3^+	obscured by primary ion beam ^b				

^aFrom Ref. 19.

^bThis was omitted from Ref. 19: F. W. Lampe (private communications).

TABLE IV. Free energies of reaction for H/D exchange.

Reactants	Product ion	ΔG_{rxn} (kcal/mol)
$\text{SiH}_3^+ + \text{SiD}_4$	SiH_3^+	0
	SiH_2D^+	-1.63
	SiHD_2^+	-1.89
	SiD_3^+	-0.75
$\text{SiH}_2\text{D}^+ + \text{SiD}_4$	SiH_2D^+	0
	SiHD_2^+	-0.88
	SiD_3^+	-0.49
$\text{SiHD}_2^+ + \text{SiD}_4$	SiHD_2^+	0
	SiD_3^+	-0.15
$\text{SiD}_3^+ + \text{SiH}_4$	SiD_3^+	0
	SiHD_2^+	-1.58
	SiH_2D^+	-1.98
	SiH_3^+	-0.99
$\text{SiHD}_2^+ + \text{SiH}_4$	SiHD_2^+	0
	SiH_2D^+	-0.85
	SiH_3^+	-0.58
$\text{SiH}_2\text{D}^+ + \text{SiH}_4$	SiH_2D^+	0
	SiH_3^+	-0.19

counts for 70% of the reactivity of SiH_3^+ with SiH_4 at room temperature.

The overall hydride exchange reaction rate of SiH_3^+ with SiH_4 significantly alters the estimated mobility of SiH_3^+ in silane plasmas. Our estimate of $340 \text{ cm}^2 \text{ Torr/V s}$ for the low field mobility of SiH_3^+ ($T = 298 \text{ K}$, thermal velocities) is much smaller than the current estimate of $1180 \text{ cm}^2 \text{ Torr/V s}$. This change increases the predicted concentration of SiH_3^+ and its reaction progeny in the silane plasma.

ACKNOWLEDGMENTS

We wish to thank T. M. Mayer and F. W. Lampe for helpful discussions regarding their ion beam studies.

- ¹ M. J. Kushner, *J. Appl. Phys.* **63**, 2532 (1988).
- ² M. E. Coltrin, R. J. Lee, and J. A. Miller, *J. Electrochem. Soc.* **131**, 425 (1984).
- ³ C. A. DeJoseph, Jr., P. D. Haaland, and A. Garscadden, *IEEE Trans. Plasma Sci.* **14**, 165 (1986).
- ⁴ H. Chatham and A. Gallagher, *J. Appl. Phys.* **58**, 159 (1985).
- ⁵ F. C. Eversteijn, *Philips Res. Rep.* **26**, 134 (1971).
- ⁶ *VLSI Technology*, edited by S. M. Sze (McGraw-Hill, New York, 1983).
- ⁷ M. L. Mandich, W. D. Reents, Jr., and M. F. Jarrold, *J. Chem. Phys.* **88**, 1703 (1988).
- ⁸ M. L. Mandich and W. D. Reents, Jr., *J. Chem. Phys.* **90**, 3121 (1989).
- ⁹ W. D. Reents, Jr. and M. L. Mandich, *J. Phys. Chem.* **92**, 2908 (1988).
- ¹⁰ M. L. Mandich, W. D. Reents, Jr., and K. D. Kolenbrander, *J. Chem. Phys.* **92**, 437 (1990).
- ¹¹ *The Mobility and Diffusion of Ions in Gases*, edited by E. W. McDaniel and E. A. Mason (Wiley, New York, 1973).
- ¹² K. Raghavachari, *J. Chem. Phys.* **92**, 452 (1990).
- ¹³ For details on this correction, see Refs. 7-10.
- ¹⁴ R. A. Alberty and W. G. Miller, *J. Chem. Phys.* **26**, 1231 (1957).
- ¹⁵ Details of phase space theory can be found in W. J. Chesnavich and M. T. Bowers, *Progr. React. Kinet.* **11**, 137 (1982); in *Gas Phase Ion Chemistry*, edited by M. T. Bowers (Academic, New York, 1979), Vol. 1.
- ¹⁶ Applications of phase space theory to ion-molecule reactions in the silane system have been previously reported: M. L. Mandich, W. D. Reents, Jr., and M. F. Jarrold, *J. Chem. Phys.* **88**, 1703 (1988); M. L. Mandich and W. D. Reents, Jr., *ibid.*, **90**, 3121 (1989).
- ¹⁷ A. Heinglein, *Kinematics of Ion-Molecule Reactions*, in *Fasci molecolari e cinetica delle reazioni*, edited by Ch. Schlier (Academic, New York, 1970), pp. 139-183.
- ¹⁸ A. Heinglein, *J. Phys. Chem.* **76**, 3883 (1972).
- ¹⁹ T. M. Mayer and F. W. Lampe, *J. Phys. Chem.* **78**, 2195 (1974).
- ²⁰ T. M. Mayer and F. W. Lampe, *J. Phys. Chem.* **78**, 2429 (1974).
- ²¹ T. M. Mayer and F. W. Lampe (private communications).
- ²² The ion velocity in our experiments has a Boltzmann distribution for 300 K. This is not appropriate for Eq. (20) which requires a reaction rate for a single velocity. We have used the rms velocity to estimate Q and the low field mobility.
- ²³ K. Raghavachari (private communications).